fortune Journals

Research Article

FORTUNE JOURNAL OF HEALTH SCIENCES

ISSN: 2644-2906

Comprehensive Profiling of The Immune Status of A Broad Range of *in vivo* Syngeneic Models to Support IO Development and to Accurately Predict Clinical Benefit of Therapy

Wentao Li, Jinghui Xiu, Liang Yao, Qiuliang Li, Guannan Li, Xiaodong Li, Lu Zhang, Chunhong Ning, Wei Yun, Shizong Hu, Jingqi Huang*

Abstract

Recently, with the approval of anti-PD-1 and anti-PD-L1 antibodies in clinical oncology, immunotherapy has changed the approach to cancer treatment and joins chemotherapy, radiation, and surgery as treatment options. Murine syngeneic tumor models are critical to the development of novel immuno-based therapy. Understanding the nature of the immune status and the tumor microenvironment of in vivo tumor models is essential to explore immunotherapy. However, the translational relevance of differences between the models is not fully understood. Therefore, we extensively characterized various murine syngeneic tumor models, which revealed striking differences in immune status and in tumor microenvironment. These findings will contribute to the appropriate selection of preclinical models for target validation and drug development. In this study, 49 tumor models over a broad range of tumor cell types, as well as corresponding in vivo syngeneic models, were intensively studied for their immune status under two conditions: tumor volume of 100 mm^3 or tumor volume between 500 to 600 mm^3. Immune status was determined by measuring T cell status and levels of immune-suppression via FACS analysis of the population of tumor-infiltrating leukocytes (TILs), $CD45^+$ T cells, $CD4^+$ T cells, $CD8^+$ T cells, T regulatory cells (Tregs), myeloid-derived suppressor cells (MDSCs), and macrophages. Furthermore, the expression of immune-related genes was analyzed by RT-PCR. Profiling data revealed the expression of these genes was different for different tumor models. We believe that this profiling data will help many scientists to properly select the correct model to support research and development, and better understand how immunotherapy agents act on the immune system.

Keywords: Dyngeneic model, Tumor, Immunotherapy, Tumor microenvironment

Introduction

Recent clinical successes in treating tumors with immunotherapies, including the application of anti-PD1, anti-PD-L1, and anti-CTLA-4 antibodies, demonstrate the potential to transform treatment methods and improve patient outcomes [1-3]. In particular, PD-1 blockade in PD-L1-expressing tumor cells can overcome immunosuppressive mechanisms present in the tumor microenvironment and reactivate tumor-specific T cells. Priming of naïve T cells into antigen-specific effector T cells requires the participation of the T cell receptor (TCR), antigen recognition, and the proper balance between expression of co-stimulatory molecules that activate T cell proliferation, and co-inhibitory molecules that attenuate T cell activation.

Affiliation:

Department of Pharmacology, Pharmaron Beijing, Co. Ltd., No. 6, TaiHe Road, BDA, Beijing, 100176, People'sRepublic of China

***Corresponding author:**
Jingqi Huang, SVP. Pharmacology; IACUC, Chair, Pharmaron Beijing, Co. Ltd. Beijing, China.

Citation: Wentao Li, Jinghui Xiu, Liang Yao, Qiuliang Li, Guannan Li, Xiaodong Li, Lu Zhang, Chunhong Ning, Wei Yun, Shizong Hu, Jingqi Huang. Comprehensive Profiling of The Immune Status of A Broad Range of *in vivo* Syngeneic Models to Support IO Development and to Accurately Predict Clinical Benefit of Therapy. Fortune Journal of Health Sciences. 7 (2024): 288-298.

Received: May 22, 2024
Accepted: May 29, 2024
Published: June 05, 2024

Li W, et al., Fortune J Health Sci 2024
DOI:10.26502/fjhs.188

Therefore, a promising strategy involves the manipulation of co-stimulatory and co-inhibitory molecules to change the balance within the tumor microenvironment from an immunosuppressive state to an immunostimulatory state. These treatments represent a shift in the approach to cancer therapy as they do not target tumor cells but instead target the immune system to escape inhibitory pathways that attenuate effective antitumor immune responses. However, despite these improvements, clinical responses are still limited. A major factor hindering these novel therapies is the complicated tumor microenvironment, and most likely, the establishment of an immunosuppressive tumor microenvironment due to the existence of Tregs and MDSCs. In many experimental models, Tregs locally regulate the interactions between cytotoxic T lymphocytes (CTLs) and antigen presenting cells (APCs) to induce CTL dysfunction by altering the balance of costimulatory and coinhibitory signals [4]. Tregs can also negatively modulate the activity of other immune cells through the action of soluble molecules, such as IL-10, IL-35, and TGF-β. Thus, it is advantageous for tumors to express membrane bound T cell inhibitory molecules and promote the expansion of Tregs against tumor antigens to evade the immune system.

Currently, murine syngeneic tumor models are the first choice for the development of immune therapeutic agents in the oncology field. Therefore, fully understanding and selecting appropriate preclinical models for target validation, and providing preclinical proof of concept for candidate immunotherapeutic drugs, is crucial to developing new therapeutic approaches for cancer treatment [5]. However, to date, the majority of studies have been performed in a small number of models (compared to xenografts) and, despite their widespread use, little is known about the genotypes and phenotypes of these syngeneic murine tumor models [6]. Consequently, a better understanding of these models is required to select appropriate models and permit both data interpretation and extrapolation to the clinic [6,7]. Here, we describe a comprehensive characterization of gene expression and immunological composition of several murine syngeneic tumor models. We found that immunosuppressive cell types predominated in syngeneic murine tumor models, and further investigation showed differences in both the composition and magnitude of tumor immune infiltrates. In conclusion, this study conducted an extensive immune status profiling of a panel of murine tumor cell lines and of commonly used syngeneic tumor models using RT-PCR and flow cytometer (FACS). Both immune-related genes and the activation of immune infiltration cells were analyzed on all validated in vivo syngeneic models. These data can be readily applied to expedite the discovery and development of novel immunotherapies by increasing the efficiency of preclinical drug development.

Materials and Methods

Cell lines and reagents

Forty-nine murine tumor cell lines were purchased from ATCC, ECACC, Shanghai Zishi, Shanghai huiying biological technology, Institute of Basic Medical Sciences, Chinese Academy of Medical Sciences or COBIOER for oncology research purposes (Table 1). Cells were cultured in their respective mediums at 37°C in an incubator with humidified atmosphere of 5% CO_2. Antibodies used for FACS analysis were purchased from Bio-Legend and Ebioscience, and RT-PCR primers and reagents were purchased from QIAGEN and Thermo Fisher. The cell culture medium RPMI 1640, DMEM, Waymouth's MB 752/1, L-15, IMDM, MEM, Fischer's, f12K are from Gibco. Anti PD-1 antibody (CD279, clone RMP1-14) was purchased from Bio-X-Cell.

RT-PCR

Tumor tissues were collected and homogenized, and total RNA was extracted with the RNA easy kit (QIAGEN). cDNA was synthesized by using a reverse transcriptase kit (Invitrogen). The data were calculated with 2-ΔCt method.

Animals

At the end of study, all the animals were terminated by carbon dioxide (CO2) euthanasia, animals were put in a 12-liter chamber with 50% volume displacement per minute for 3 minutes, CO2 flow was maintained for 1 minute after respiratory arrest to confirm the death of animal. All animal studies were performed according to the guidelines approved by the IACUC and the guidance of the Association for AAALAC. The Animal Use Protocol (AUP) ON-SYN-06012023 was approved by Pharmaron IACUC members.

The General procedures for animal care and housing were in accordance with the standard of Commission on Life Sciences, National Research Council, SOPs. Female mice aged 7 to 9 weeks with body weight between 18-22 g were purchased from Beijing Vital River Laboratory Animal Technology Co., Ltd (joint venture with Charles River Laboratories) and / or Animal Research Center of Nanjing University. Mice used for these studies were quarantined for 3 days initially, and complete health checks were performed by an experienced veterinarian. The mice were housed under specific pathogen-free conditions on a 12/12 light/dark cycle, with ad libitum UV-treated water and rodent diet. For the experimental mouse tumor model, MC38 (1 x 10^8cells/ml) or EMT6 (2 x 10^5cell/ml) were inoculated subcutaneously onto the right flank of the mice. Twice a week (BIW), 2.5 mg/kg or 10 mg/kg anti-PD-1 antibody (Bio-X-Cell) or vehicle PBS were injected intraperitoneally. Tumor volume was measured via caliper and calculated using the formula (a^2 width × b length)/2. Tumor volume was used to calculate

Citation: Wentao Li, Jinghui Xiu, Liang Yao, Qiuliang Li, Guannan Li, Xiaodong Li, Lu Zhang, Chunhong Ning, Wei Yun, Shizong Hu, Jingqi Huang. Comprehensive Profiling of The Immune Status of A Broad Range of *in vivo* Syngeneic Models to Support IO Development and to Accurately Predict Clinical Benefit of Therapy. Fortune Journal of Health Sciences. 7 (2024): 288-298.

Li W, et al., Fortune J Health Sci 2024
DOI:10.26502/fjhs.188

Table 1: Cell lines and culture conditions

Cell Line	Source	Mouse Strain	Tissue	Culture Medium
MB49	Shanghai Zishi	C57BL/6	Bladder cancer	RPMI 1640+10%FBS
MBT-2	Shanghai Zishi	C3H	Bladder cancer	DMEM+10%FBS
4T1	ATCC	BALB/c	Breast cancer	RPMI 1640+10%FBS
EMT6	ATCC	BALB/c	Breast cancer	Waymouth's MB 752/1 Medium with 2mM L-glutamine+15%FBS
Ac711	ATCC	DBA/2	Breast cancer	DMEM+10%FCS
JC	ATCC	BALB/c	Breast cancer	RPMI 1640+10%FBS
TC-1	Shanghai huiying biological technology	C57BL/6	Cervical cancer	DMEM + 10% FBS
Colon26	COBIOER	BALB/c	Colon cancer	RPMI 1640+10%FBS
CT26	ATCC	BALB/c	Colon cancer	RPMI 1640+10% FBS
MC38	COBIOER	C57BL/6	Colon cancer	RPMI 1640+10% FBS
RENCA	ATCC	BALB/c	Kidney cancer	RPMI 1640 + 10%FBS + 0.1mM NEAA + 0.1mM NaP + 2mM Glutamine
MOPC-31C	ATCC	BALB/c	Leukemia	L-15+20%FBS+0.2mM L-glutamine
P3.6.2.8.1	ATCC	BALB/c	Leukemia	DMEM+10%FBS
WEHI-3	ATCC	BALB/c	Leukemia	IMDM+10% FBS+0.05 mM 2-mercaptoethanol
C1498	ATCC	C57BL/6	Leukemia	DMEM + 10% FBS
L1210	COBIOER	DBA/2	Leukemia (lymphocytic)	DMEM + 10% FBS
Sai/N	ATCC	A/Jax	Fibrosarcoma	IMDM+10%FBS
WEHI-164	ATCC	BALB/c	Fibrosarcoma	RPMI 1640+10% FBS
GL-261	COBIOER	C57BL/6	Glioblastoma	RPMI 1640+10% FBS
H22	COBIOER	BALB/c	Liver cancer	RPMI 1640+10%FBS
HEPA1-6	ATCC	C57BL/6	Liver cancer	DMEM+10% FBS
KLN-205	ATCC	DBA/2	Lung cancer	MEM + 10% FBS + NEAA
LL2	ATCC	C57BL/6	Lung cancer (LLC)	DMEM+10% FBS
P388D1	ATCC	DBA/2	Lymphoma	RPMI 1640+10% FBS
EL-4	ATCC	C57BL/6	Lymphoma (T lymphocyte)	DMEM+10% FBS
A20	ATCC	BALB/c	Lymphoma (B lymphocyte)	RPMI 1640+10% FBS + 2mM Glutamine
B16	ATCC	C57BL/6	Melanoma	EMEM+10%FBS(Gibco)
B16F10	ATCC	C57BL/6	Melanoma	DMEM+10% FBS
J558	ATCC	BALB/c	Myeloma	DMEM+10%FBS
Sarcoma 180	ATCC	DBA/2	Sarcoma (ascites)	DMEM+10%FBS
CM3	ATCC	DBA/2	Skin cancer	DMEM + 10% FBS
MLTC-1	ATCC	C57BL/6	Testis cancer (Leydig cell)	RPMI 1640+10% FBS
Eph4.1424	COBIOER	DBA/2	Breast cancer	DMEM + 10% FBS
L5178-R(LY-R)	ATCC	BALB/c	Lymphoma (thymic lymphoma)	Fischer's medium with 0.1 g/L sodium pyruvate and 1.125 g/L sodium bicarbonate + 10% HoS
MOPC-315	ATCC	BALB/c	Myeloma (plasmacytoma)	DMEM + 10% FBS
PY8119	ATCC	C57BL/6	Breast cancer	f12K+Fetal Clone II Serum, 5%
T27A	ATCC	BALB/c	Leukemia	RPMI 1640+10%FBS+2 mM L-glutamine +1.5 g/L sodium bicarbonate+4.5 g/L glucose+10 mM HEPES+1.0 mM sodium pyruvate +0.05 mM 2-mercaptoethanol

Citation: Wentao Li, Jinghui Xiu, Liang Yao, Qiuliang Li, Guannan Li, Xiaodong Li, Lu Zhang, Chunhong Ning, Wei Yun, Shizong Hu, Jingqi Huang. Comprehensive Profiling of The Immune Status of A Broad Range of *in vivo* Syngeneic Models to Support IO Development and to Accurately Predict Clinical Benefit of Therapy. Fortune Journal of Health Sciences. 7 (2024): 288-298.

B16F0	ATCC	C57BL/6	Melanoma	DMEM+10%FBS
B16-F1	ATCC	C57BL/6	Melanoma	DMEM+10% FBS
CT26.CL25	ATCC	BALB/c	Colon Carcinoma	RPMI 1640+10% FBS + NEAA+0.4mg/ml G418
FO	COBIOER	BALB/c	Plasmacytoma	DMEM + 10% FBS
K7M2 wt	ATCC	BALB/c	Osteosarcoma	DMEM + 10% FBS
MPC-11	ATCC	BALB/c	Myeloma (Plasmacytoma)	DMEM+10% HoS
N1E115	ATCC	BALB/c	Neuroblastoma	DMEM + 10% FBS
N1E115-1	ECACC	BALB/c	Neuroblastoma	DMEM + 10% FBS + Glu
P3X63Ag8U.1	ATCC	BALB/c	Myeloma (plasmacytoma)	DMEM + 10% FBS
PANC02	Institute of Basic Medical Sciences, Chinese Academy of Medical Sciences	C57BL/6	Pancreatic cancer (pancreatic ductal adenocarcinoma)	DMEM+5%FBS
RM-1	COBIOER	C57BL/6	Prostate cancer	DMEM + 10 % FBS
D1B	ATCC	DBA/2	Leukemia	RPMI 1640+10%FBS+2 mM L-glutamine +1.5 g/L sodium bicarbonate+4.5 g/L glucose+10 mM HEPES+1.0 mM sodium pyruvate +0.05 mM 2-mercaptoethanol

tumor growth inhibition (TGI), an indicator of antitumor effectiveness, using the formula: TGI = (1-T/C) × 100%, where "T" and "C" were the mean relative volumes (% tumor growth) of the tumors in the treated and the control groups, respectively.

Tissue dissociation and cytometric analysis

After the tumor volumes reached ~100mm^3 and ~500mm^3, tumor tissues were harvested and processed using a tumor dissociation enzyme mix. The cell suspensions were passed through 70 µm and 40 µm cell strainers and resuspended FACS buffer (PBS supplemented with 2% FBS). Cells were transferred into FACS tubes and blocked with anti-CD16/32 mAb, then stained with an antibody cocktail including anti-mouse CD45 (PerCP-Cy5.5, Biolegend), CD4 (PE/CY7, Biolegend), CD3 (APC, Biolegend), CD8 (BV510, Biolegend), CD11b (FITC, ebioscience), Gr-1 (BV510, Biolegend), F4/80 (BV421, Biolegend), and CD11c (PE, ebioscience) antibodies for 20 min at 4°C. Cells were then resuspended in 2 ml of fixation buffer and 1× permeabilization buffer was added along with add 2 ul of FOXP3 Abs, and incubated at 4°C for 30 mins in the dark. Next, fixed cells were washed with 1× intracellular buffer, centrifuged at 600 rpm at 4°C, and incubated with anti-mouse FoxP3 antibodies (PE, ebioscience). For each sample, 100,000 live events were collected using a BD Canto Cytometer. The data were analyzed with BD FACSDiva™ software.

Statistical analyses

Flow cytometry data was analyzed in GraphPad Prism using one-way ANOVA with Tukey's correction for multiple comparisons. For tumor growth studies, group sizes were determined using power analyses based on the variability of the models in pilot studies. Tumor growth data were log10 transformed [8, 9]. Models were defined as having statistical significance if the growth kinetics P value between the treated group and the control group was <0.05.

Results

Cell line and culture condition

Expression levels and correlation of PD-L1 and MHCI

Tumors often exploit immune-checkpoint pathways, such as the PD-1 pathway, to protect themselves from the antitumor immune response. PD-L1, the ligand of PD-1, is frequently upregulated on various types of tumor cells, where it inhibits local antitumor T cell responses. To explore the expression levels and correlation of PD-L1 and MHCI on the murine cancer cell lines, we used flow cytometry. The results showed heterogeneity in PD-L1 and MHCI expression across different murine tumor cell lines (Fig. 1A and 1B) and a positive correlation was found between PD-L1 and MHCI expression in cancer cell lines (R^2 square=0.6157, ***P<0.0001) (Fig. 1C). To determine whether differences in tumor immune infiltration cells could affect responsiveness to immune-checkpoint blockade, we analyzed the expression level of immune-related pathway factors by RT-PCR in various tumor models. We found heterogeneity in tumor immune infiltrates across different tumor cell lines and across murine syngeneic models (Fig. 1 and Fig. 2).

Immune marker expression as readout of immune pathway activity

In a second study, we examined the activity of immune-related pathways in tumor immune infiltrates. To this end, we used RT-PCR to analyze the expression level of immune-relevant proteins, such as regulatory T cell-related proteins, proteins relevant to tumor associated macrophages (TAM),

Li W, et al., Fortune J Health Sci 2024
DOI:10.26502/fjhs.188

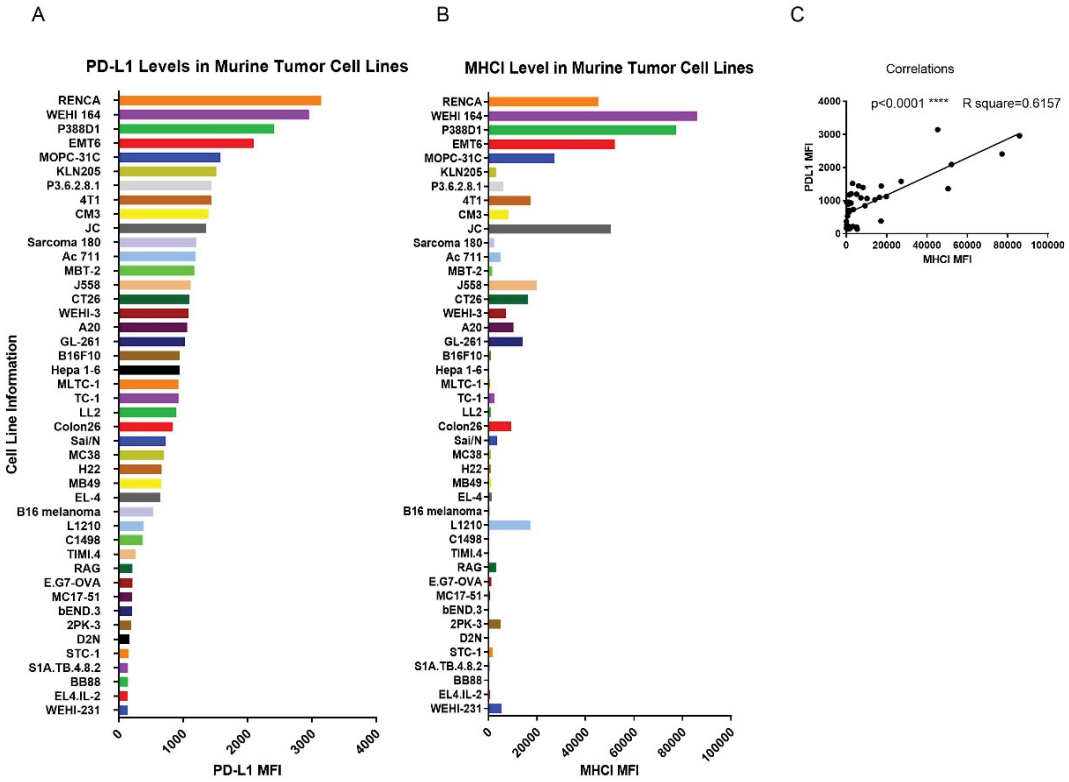

Figure 1: FACS analysis of PD-L1 and MHCI levels in multiple murine tumor cell lines

Murine tumor cell lines (total 44 cell lines) were analyzed by flow-cytometer for PD-L1 (A) and MHCI (B) expression, and the correlation between PD-L1 and MHCI levels was reported (R^2=0.6157, ***P<0.0001) (C).

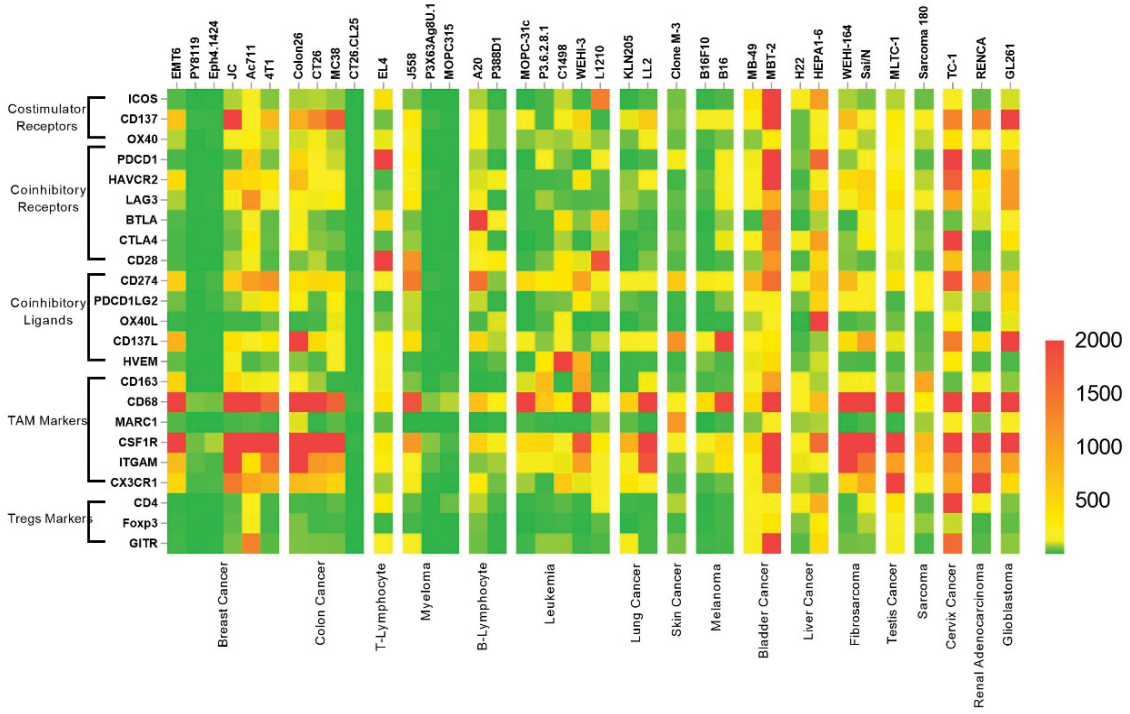

Figure 2: Gene expression of immune-related pathways in murine syngeneic models

The expression of immune-related genes was analyzed by RT-PCR (Fig. 2) on 37 different tumor models covering 17 tumor types. A total of 23 immune-related genes corresponding to co-stimulatory receptors, co-inhibitory receptors, TAM markers, and Tregs markers were evaluated, with high amplification shown as light red colors, middle amplification as yellow colors, and low amplification as dark green colors.

Citation: Wentao Li, Jinghui Xiu, Liang Yao, Qiuliang Li, Guannan Li, Xiaodong Li, Lu Zhang, Chunhong Ning, Wei Yun, Shizong Hu, Jingqi Huang. Comprehensive Profiling of The Immune Status of A Broad Range of *in vivo* Syngeneic Models to Support IO Development and to Accurately Predict Clinical Benefit of Therapy. Fortune Journal of Health Sciences. 7 (2024): 288-298.

Li W, et al., Fortune J Health Sci 2024
DOI:10.26502/fjhs.188

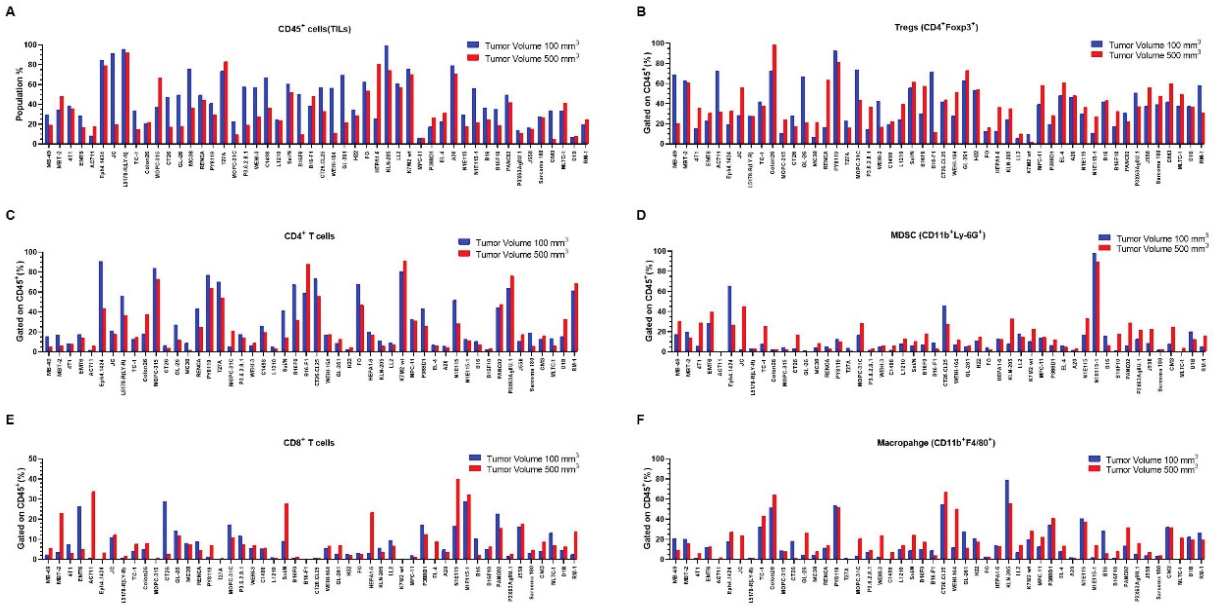

Figure 3: Population of immune cell populations in tumor tissues (tumor volume: 100 mm^3 and 500 mm^3)

Flow cytometry analysis was used to determine the percentages of immune cells in different volumes of tumor tissues of multiple tumor cell lines (Fig. 3), including the percentages of $CD45^+$ cells (Fig. 3A), Tregs (Fig. 3B), $CD4^+$T cells (Fig. 3C), MDSCs (Fig. 3D), $CD8^+$ T (Fig. 3E), and macrophages (Fig. 3F).

co-stimulator receptors of T cells, co-inhibitory receptors of T cells, and co-inhibitory ligands of tumor cells. The results showed a large variety in the expression of immune markers (Fig. 2). The expressions of TAM-related markers were relatively high, which indicated that the tumor microenvironment was immunosuppressive. Immunological diversity broadly uncovers the diversity of tumor models and therefore provides a powerful resource to evaluate different immunotherapies in the context of these distinct microenvironments for preclinical application.

FACS analysis of immune cell populations in tumor tissues reveals heterogeneity across murine syngeneic models

A complicated immune microenvironment within a tumor often leads to a poor prognosis. Interactions between cancer cells and other immune cell populations contribute to the establishment of an immunosuppressive system that promotes the growth of the tumor. To explore the immune status of tumors, we used flow cytometry to analyze the tumor immune cell infiltration across murine models. Tumors were collected at an average volume of 100 mm^3 and 500 mm^3 approximately, as this often corresponds to the tumor volume at initiation of dosing in efficacy studies. Immune phenotyping profiling revealed profound differences in the tumor microenvironment across different tumor cell lines in multiple tumor syngeneic models. With the growth of tumor volume, the population of immune cells in tumor tissues showed definite heterogeneity. The ratio of $CD4^+$T/$CD8^+$T cells was reduced in general with tumor growth, and Tregs and MDSCs were increased in most tumor cell lines (Fig. 3), demonstrating that the reduction of tumor-infiltrating lymphocytes and the increase of immunosuppressive cells in the tumor microenvironment might have contributed to tumor growth.

Efficacy of PD-1 mAb and CTLA-4 mAb treatment in murine syngeneic models

Table 2 shows TGI of anti-PD-1 antibody treatment in different syngeneic models. We observed various therapeutic effects of anti-PD-1 antibody in different tumor models. Some tumor models showed a high response to anti-PD-1 antibody, while other tumor models showed a mild response or no response. These results serve to identify reference models that can be used for anti-PD-1 applications or to identify possible models for the development of combination therapy in research and development, and clinical treatment.

Immune-modulating effects of PD-1 inhibition on the MC38 murine colon cancer and EMT6 murine breast cancer models

Immune checkpoint blocking therapy is currently approved by the FDA to treat multiple cancer types. PD-1 is overexpressed on TILs and the PD-1 ligand is highly up-regulated in most cancer cells. Therefore, we chose the relatively highly responsive colon model MC38 and the moderately responsive breast cancer model EMT6 for further study. We assessed the antitumor activity of PD-1 antibody in

MC38 tumor models. The results showed that TGI followed anti-PD-1 (2.5 mg/kg) treatment in the MC38 model with a TGI of 54% (Fig. 4), with no significant change in mean body weight during the treatment period. We detected immune cell populations ($CD45^+$, $CD3^+$, $CD4^+$, $CD8^+$, Tregs, MDSCs) via flow cytometry on Day 0 (with the vehicle control mean tumor volume approximately 100 mm^3) and Day 7 (mean tumor volume approximately 500-600 mm^3) of treatment. We also analyzed the expressions of immune pathway-related genes on Day 0 and Day 7. Expression levels of immune pathway-related genes identified through flow cytometry were investigated using RT-PCR as described above. Flow cytometry results revealed that $CD4^+$ T cells were significantly increased on Day 7 with anti-PD-1 treatment compared to the control group ($P<0.05$). Levels of other immune cells ($CD45^+$, $CD8^+$, Tregs) were decreased, and immunosuppressive MDSCs had no obvious changes compared to the control group. The TAM- and Tregs-related gene expression levels were decreased in general, and gene expression levels of co-stimulator receptors, co-inhibitory receptors of T cells, and co-inhibitory ligands of tumor cells, were increased in the anti-PD-1 treated group compared to the control group.

Table 2: TGI of PD-1 check point inhibitors

Disease	Tumor Model	PD-1 mAb TGI %	Dose(mg/kg)
Breast	JC	~ 10%	10
	Ac 711	10% ~ 30%	5
	4T1	~ 10%	10
	EMT6	10% ~ 30%	10
	PY8119	~ 0%	5
	Eph4.1424	60% ~ 80%	5
Colon	Colon26	20% ~ 40%	10
	CT26	20% ~ 50%	10
	CT26.CL25	~10%	5
	MC38	50%~80%	2.5~10 mg/kg
Lung	KLN-205	10% ~ 30%	10
	LLC	~ 10%	10
Melanoma	B16F10	~ 20%	10~15
	B16	30% ~ 50%	10
	B16F0	~ 0%	5
	B16F1	~10%	5
	B16-OVA	~10%	5
Myeloma	MOPC315	~ 0%	10
	P3X63Ag8U.1	~ 0%	5
	MPC-11	~ 0%	5
	J558	~ 0%	5
Bladder	MB49	45% ~ 65%	10
	MBT-2	60% ~ 80%	5
Pancreatic cancer	PANC02	~ 0%	10
Liver	H22	40% ~ 60%	10
	BNL 1ME A.7R.1	~ 0%	10
Brain (Glioma)	GL261	40% ~ 60%	5
Fibrosarcoma	WEHI 164	40% ~ 60%	10
B Lymphocyte	A20	35% ~ 55%	10
Leukemia	C1498	35% ~ 55%	5
	L1210	~ 0%	10
	D1B	~ 0%	10
	WEHI-3	40% ~ 60%	10
	T27A	~ 0%	5
	MOPC-31C	~ 0%	10
	P3.6.2.8.1	~ 0%	5
Lymphoma	EL-4	~10%	5
	P388D1	~ 0%	5
	L5178-R	~ 0%	5
	E.G7-OVA	10% ~ 30%	5
Neuroblastoma	N1E115	~30%	10
	N1E115-1	~ 0%	10
	Neuro-2a	~ 0%	5
Others	Sarcoma 180 (Sarcoma)	~ 35%	10
	TC-1 (cervix)	~ 0%	10
	RENCA (Renal)	20% ~ 40%	10
	FO (Plasmacytoma)	~ 0%	10
	RM-1 (Prostate)	~ 10%	10
	CM3 (Skin)	~ 0%	5

TGI by anti-PD-1 (10 mg/kg) treatment in the EMT6 model was 23% (Fig. 5), with no remarkable changes in the mean body weight of mice during the treatment period. Flow cytometry results showed that the percentage of $CD4^+$ T cells/ $CD8^+$ T cells was significantly increased following anti-PD-1 treatment compared to the control group (*$P<0.05$), MDSCs and Tregs were significantly decreased, and $CD45^+$, $CD3^+$ T cells were increased compared to the control groups on Day 8. The expression of gene for TAM markers, Tregs markers, co-stimulator receptors, co-inhibitory receptors of T cells, and co-inhibitory ligands of tumor cells were all increased. These results showed that immunosuppression in the tumor microenvironment improved through anti-PD-1 treatment. At the same time, our data illustrated the remarkable differences of tumor microenvironments in different tumor models, which depends on the tumor type and the progression of tumor growth. Multiple tumors showed infiltrated immune cells which reflected the composition and magnitude of phenotypes of infiltrates and might have contributed to the

Li W, et al., Fortune J Health Sci 2024
DOI:10.26502/fjhs.188

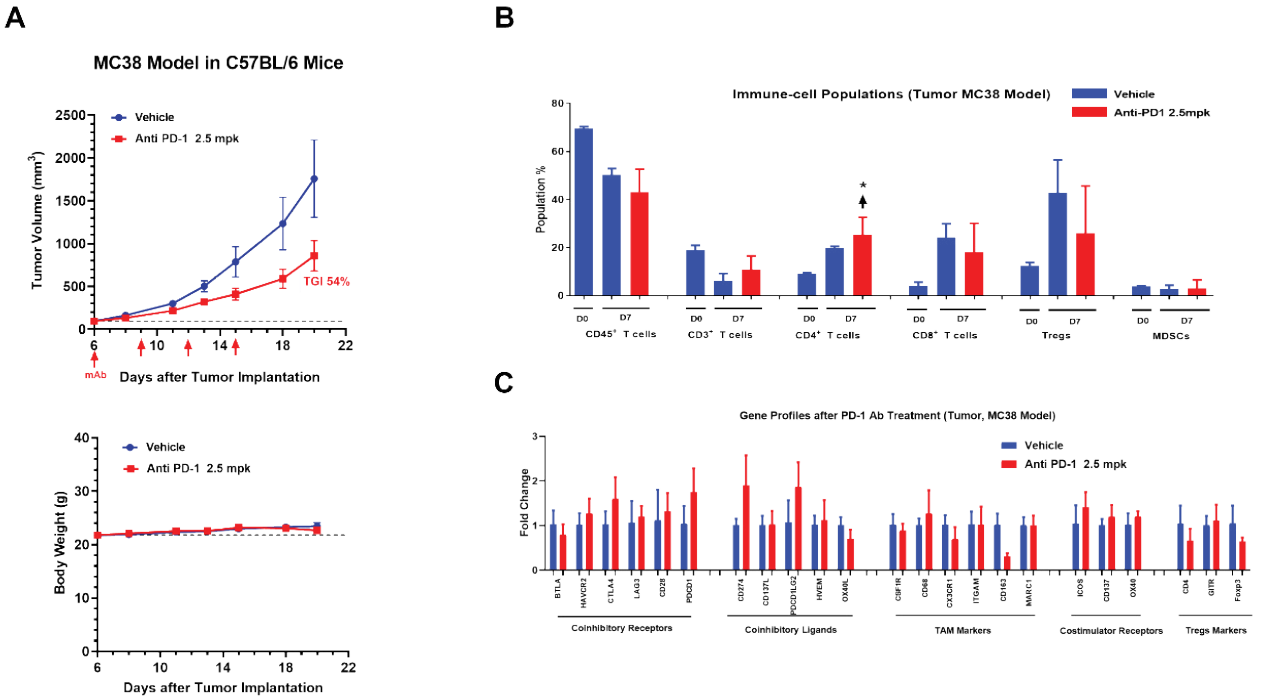

Figure 4: The antitumor activity of anti-PD-1 treatment varies for the MC38 murine colon cancer model

Tumor growth curves for MC38 subcutaneous murine syngeneic tumor model treated with PD-1 antibody 2.5 mg/kg (CD279, clone RMP1-14). Treatment was given by intraperitoneal injection on the days marked with ticks on the x axis of the graphs (Fig. 4A). MC38 tumors were collected on Day 7 post treatment for FACS analysis for immune cell profiling (Fig 4B). Gene profiling of the tumor was conducted (Fig 4C). n ≥ 6 mice per group. *P <0.05, ns: non-significant P ≥0.05.

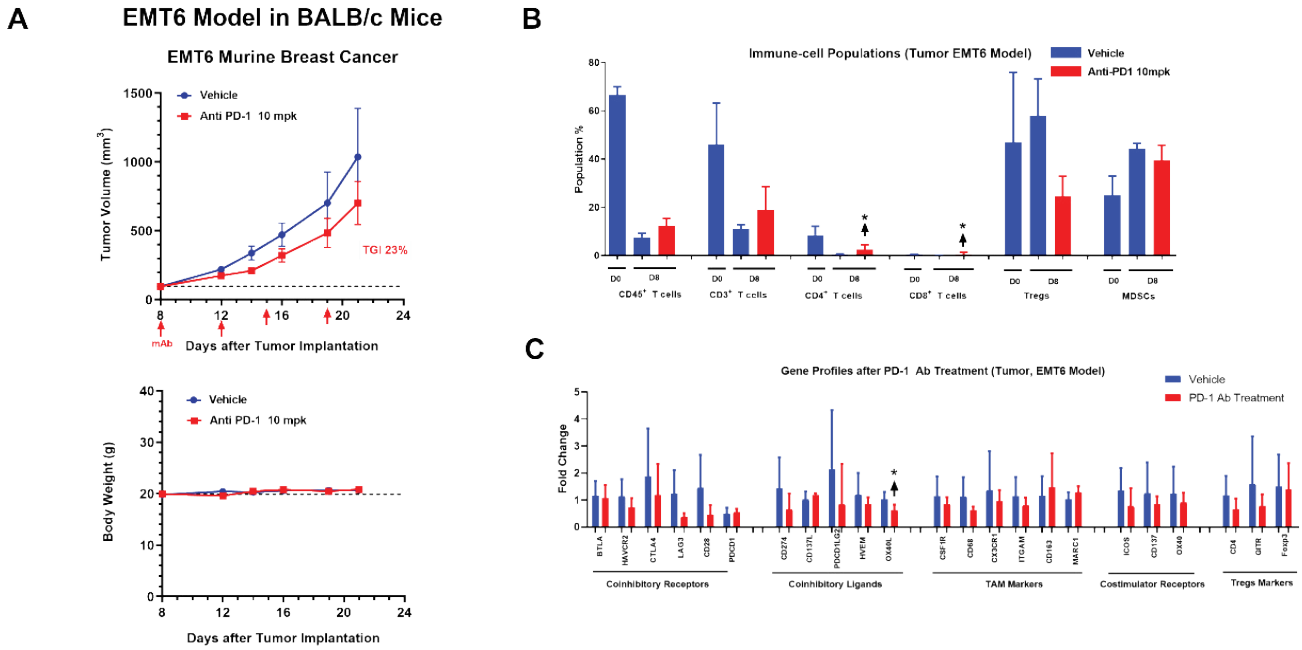

Figure 5: Anti-tumor effect of PD-1 antibody on EMT6 murine breast cancer model

*Tumor growth curves for EMT6 subcutaneous murine syngeneic tumor model treated with (A) PD-1 antibody 10 mg/kg (CD279, clone RMP1-14). Treatment was also given by intraperitoneal injection on the days marked with ticks on the x axis of the graphs (Fig 5A). EMT6 tumors were collected on Day 8 of treatment for FACS analysis for immune cell profiling (Fig 5B). Gene profiling of the tumor was conducted (Fig 5C). n ≥ 6 mice per group. *P <0.05, ns: non-significant P ≥0.05*

Citation: Wentao Li, Jinghui Xiu, Liang Yao, Qiuliang Li, Guannan Li, Xiaodong Li, Lu Zhang, Chunhong Ning, Wei Yun, Shizong Hu, Jingqi Huang. Comprehensive Profiling of The Immune Status of A Broad Range of *in vivo* Syngeneic Models to Support IO Development and to Accurately Predict Clinical Benefit of Therapy. Fortune Journal of Health Sciences. 7 (2024): 288-298.

Li W, et al., Fortune J Health Sci 2024
DOI:10.26502/fjhs.188

alteration of differential gene expression related to immune pathways. In addition, these data highlight the need for extensive characterization of models used for preclinical immunotherapy research, and provides data that will, based on the proposed mechanism of action of the therapy being evaluated, support investigators in selecting appropriate models using hypothesis-driven rationales.

Tumor growth curves for MC38 subcutaneous murine syngeneic tumor model treated with PD-1 antibody 2.5 mg/kg (CD279, clone RMP1-14). Treatment was given by intraperitoneal injection on the days marked with ticks on the x axis of the graphs (Fig. 4A). MC38 tumors were collected on Day 7 post treatment for FACS analysis for immune cell profiling (Fig 4B). Gene profiling of the tumor was conducted (Fig 4C). $n \geq 6$ mice per group. *$P < 0.05$, ns: non-significant $P \geq 0.05$.

Discussion

Tumors not only contain cancer cells, but also comprise a rich microenvironment composed of blood vessels, APCs, neutrophils, myeloid-derived suppressor cells, tumor-associated macrophages, fibroblasts, components of the extracellular matrix, and soluble factors (such as cytokines and growth factors), all of which may assist or hinder anti-tumor immune responses. The lack of clinical efficacy of cancer therapy can be mostly attributed to an immunosuppressive tumor microenvironment, and the presence of Tregs or MDSCs, which can inhibit anti-tumor immune responses and is associated with decreased survival [10–12]. Alternatively, the expression of inhibitory molecules on the surface of tumor cells could promote the expansion and accumulation of nonresponsive anergic T cells or Tregs within the tumor microenvironment [13–16]. Murine syngeneic tumor models play a central role in the development of novel immunotherapies. Considering the limited understanding of preclinical trial models, there is a need to extensively elucidate their immunological characteristics in the tumor microenvironment. In this study, a total of 44 tumor cell lines were analyzed for the expression of PD-L1 and MHCI at the cellular level, with the highest expression on RENCA, WEHI-164, P388D, and EMT6 cells, and the lowest expression levels on EL4, LL-2, and WEHI-231 cells. The correlation of PD-L1 expression vs. MHCI expression was R^2=0.62 (Fig. 1). Immune-related genes were analyzed by RT-PCR (Fig. 2). Furthermore, 50 models were profiled for immune status when the tumor volume was ~100 mm^3 and ~500 mm^3 (Fig. 3). Herein, we provide a guide for the selection of syngeneic models to test drug therapeutic effect and to evaluate immunotherapy, which not only increases the value of such studies but also reduces the numbers of animals used in scientific research. PD-1 antibody was tested, and the response of this checkpoint inhibitor was reported with TGI values.

Immune checkpoint plays an important regulatory role in adaptive immunity and determines the fate of the immune cell towards activation or suppression, which has been extensively studied in recent years [17–19]. It was divided into two categories: forward signaling towards TC, and both forward and reverse signaling towards TC and APC. Each category can be further divided into stimulatory and inhibitory immune checkpoints. The stimulatory immune checkpoint turns up the immune system leading to immune cell proliferation or activation, while the inhibitory immune checkpoint turns down the immune system leading to immune cell suppression or death. For instance, costimulatory molecules will enhance T cell expansion and differentiation either because of increased rates of T cell proliferation or increased survival of the activated T cells [20–24]. Elucidation of the complex web of stimulatory and inhibitory signals in different models will ultimately contribute to guiding treatment strategies and enhancing therapeutic responses. In this study, we tested various costimulatory receptor and coinhibitory ligand markers in MC38 and EMT tumor syngeneic models, and also detected immunosuppressive MDSCs and Tregs, and multiple TILs in multiple syngeneic models. We observed that the composition of immune-infiltrate cells in the tumor microenvironment across the models was strikingly varied. Previous studies have shown that different syngeneic tumor models can respond differently to treatment [25, 26], so it was necessary that the differences between an extensive array of syngeneic models were characterized. A complicated immune microenvironment with tumor development leads to an unsatisfactory prognosis. This immunological variety of immune infiltration cells observed in this study broadly demonstrated the diversity of tumors observed clinically, and therefore may provide suitable settings to evaluate experimental immunotherapies in the context of these distinct microenvironments. Our data also illustrated the remarkable differences between tumor microenvironments which were influenced by the tumor type and the progression of tumor growth. Infiltrated immune cells in the tumor tissues reflected the composition and magnitude of phenotypes of infiltrates and contributed to the alteration of differential gene expression related to immune pathways. Hopefully, this profiling data with in vivo treatment of PD-1 antibody will help scientists to select appropriate models to support research and development, and to better understand how immunotherapy agents act on the immune system.

In summary, we provide an extensive range of commonly used murine syngeneic models that allow for the selection of a model based on the biology of the tumor cells and the tumor microenvironment. The integration of such data sets will inform optimal therapeutic strategies, which will contribute to a better understanding of human cancer subtypes and, in turn, may ultimately improve the efficiency of drug development for oncology.

Citation: Wentao Li, Jinghui Xiu, Liang Yao, Qiuliang Li, Guannan Li, Xiaodong Li, Lu Zhang, Chunhong Ning, Wei Yun, Shizong Hu, Jingqi Huang. Comprehensive Profiling of The Immune Status of A Broad Range of *in vivo* Syngeneic Models to Support IO Development and to Accurately Predict Clinical Benefit of Therapy. Fortune Journal of Health Sciences. 7 (2024): 288-298.

Acknowledgements

Thanks to Dr. Chune Liu, Project Manager, Pharmacology of Pharmaron Inc., for providing valuable comments and suggestions for this manuscript. Thanks to Dr. Erich Grimm, the Vice President, BD of Pharmaron Inc., for proof reading.

Statements & Declarations

This work was supported by Pharmaron Beijing, Co. Ltd. Author Jingqi Huang has received research support from Pharmacology Pharmaron Beijing, Co. Ltd.

Author Contributions

Jingqi Huang is fully responsible to the study design and data quality.

Jinghui Xiu and Shizong Hu managed ex vivo section including FACS and gene analysis.

Wentao Li, Lu Zhang, Liang Yao, Guannan Li, Qiuliang Li, Xiaodong Li and Wei Yun performed in vivo studies.

Chunhong Ning composed the manuscript.

All authors read and approved the final manuscript.

Availability of data and materials

The data generated during and analyzed during the current study are available from the corresponding author on reasonable request.

Declarations

Conflict of interest

All authors are employed by Pharmaron Beijing, Co. Ltd. This study was sponsored by Pharmacology Pharmaron Corporation.

Consent for publication

Not applicable.

Ethics approval

All in vivo experiments were conducted in Pharmaron Pharmacology with approved animal protocols. In vivo experiments were done according to the guidelines approved by the Institutional Animal Care and Use Committee (IACUC) of Pharmaron Pharmacology in accordance with all standards of the Association for Assessment and Accreditation of Laboratory Animal Care (AAALAC).

References

1. Maio M, Grob JJ, Aamdal S, Bondarenko I, Robert C, Thomas L, et al. Five-year survival rates for treatment-naive patients with advanced melanoma who received ipilimumab plus dacarbazine in a phase III trial. J Clin Oncol 33 (2015): 1191-6.
2. Brahmer J, Reckamp KL, Baas P, Crino L, Eberhardt WE, Poddubskaya E, et al. Nivolumab versus Docetaxel in Advanced Squamous-Cell Non-Small-Cell Lung Cancer. NEngl J Med 373 (2015): 123-35.
3. Herbst RS, Baas P, Kim DW, Felip E, Perez-Gracia JL, Han JY, et al. Pembrolizumab versus docetaxel for previously treated, PD-L1-positive, advanced non-small-cell lung cancer (KEYNOTE-010): a randomised controlled trial. Lancet (2015).
4. DobrowolskaH, GillKZ, SerbanG, IvanE, LiQ, QiaoP, etal. Expression of immune inhibitory receptor ILT3 in acute myeloid leukemia with monocytic differentiation. CytometryBClinCytom 84 (2013): 21–9.
5. Grosso JF, Jure-Kunkel MN. CTLA-4 blockade in tumor models: an overview of preclinical and translational research. Cancer Immun 13 (2013): 5.
6. Gould SE, Junttila MR, de Sauvage FJ. Translational value of mouse models in oncology drug development. Nat Med 21 (2015): 431-9.
7. Dranoff G. Experimental mouse tumour models: what can be learnt about human cancer immunology? Nat Rev Immunol 12 (2012): 61-6.
8. Demidenko E. Statistical comparison of color cancer cell images. Oncol Rep 15 (2006): 1077-9.
9. Heitjan DF. Biology, models, and the analysis of tumor xenograft experiments. Clin Cancer Res 17 (2011): 949-51.
10. GabrilovichDI, NagarajS. Myeloid-derived suppressor cells as regulators of the immune system. Nat RevImmunol 9 (2009): 162–74.
11. GabrilovichDI, Ostrand-RosenbergS, BronteV. Coordinated regulation of myeloid cells by tumours. NatRevImmunol 12 (2012): 253–68.
12. TengMW, RitchieDS, NeesonP, SmythMJ. Biology and clinical observations of regulatory T cells in cancer immunology. CurrTopMicrobiolImmunol 344 (2011): 61–95.
13. L Wang, K Pino-Lagos, VC de Vries, I Guleria, MH Sayegh and RJ Noelle, "Programmed death 1 ligand signaling regulates the generation of adaptive Foxp3+CD4+ regulatory T cells,"Proceedings of the National Academy of Sciences of the United States of America 105 (2008): 9331–9336.
14. A Tuettenberg, E Huter, M Hubo et al. "The role of ICOS in directing T cell responses: ICOS-dependent induction of T cell anergy by tolerogenic dendritic cells," Journal of Immunology 182 (2009): 3349–3356.

15. RJ Greenwald, VA Boussiotis, RB Lorsbach, AK Abbas, and AH Sharpe. "CTLA-4 regulates induction of anergy in vivo," Immunity 14 (2001): 145–155.

16. M Busse, M Krech, A Meyer-Bahlburg, C Hennig, and G Hansen, "ICOS mediates the generation and function of CD4+CD25+Foxp3+ regulatory T cells conveying respiratory tolerance," The Journal of Immunology 189 (2012): 1975–1982.

17. S Ostrand-Rosenberg. "CD4+ T lymphocytes: a critical component of antitumor immunity," Cancer Investigation 23 (2005): 413–419.

18. E Riquelme, LJ Carre˜no, PA Gonz′alez and AM Kalergis. "The duration of TCR/pMHC interactions regulates CTL effector function and tumor-killing capacity," European Journal of Immunology 39 (2009): 2259–2269.

19. AM Kalergis and JV Ravetch, "Inducing tumor immunity through the selective engagement of activating Fcγ receptors on dendritic cells," Journal of Experimental Medicine 195 (2002): 1653–1659.

20. PR Rogers, J Song, I Gramaglia, N Killeen and M Croft."OX40 promotes Bcl-xL and Bcl-2 expression and is essential for long-term survival of CD4 T cells," Immunity 15 (2001): 445–455.

21. AR Weatherill JR Maxwell, C Takahashi AD Weinberg and AT Vella. "OX40 ligation enhances cell cycle turnover of Ag-activated CD4 T cells in vivo," Cellular Immunology 209 (2001): 63–75.

22. AD. Holdorf, O Kanagawa and AS Shaw. "CD28 and T cell co-stimulation," Reviews in Immunogenetics 2 (2000): 175–184.

23. NJ Borthwick, M Lowdell, M Salmon, and AN Akbar. "Loss of CD28 expression on CD8+ T cells in induced by IL-2 receptor γ chain signalling cytokines and type I IFN, and increases susceptibility to activation-induced apoptosis," International Immunology 12 (2000): 1005–1013.

24. M Habib-Agahi, TT Phan and PF Searle. "Co-stimulation with 4-1BB ligand allows extended T-cell proliferation, synergizes with CD80/CD86 and can reactivate anergic T cells "International Immunology 19 (2007): 1383–1394.

25. Herbst RS, Soria JC, Kowanetz M, Fine GD, Hamid O, Gordon MS, et al. Predictive correlates of response to the anti-PD-L1 antibody MPDL3280A in cancer patients. Nature 515 (2014): 563-7.

26. Lechner MG, Karimi SS, Barry-Holson K, Angell TE, Murphy KA, Church CH, et al. Immunogenicity of murine solid tumor models as a defining feature of in vivo behavior and response to immunotherapy. J Immunother 36 (2013): 477-89.

Citation: Wentao Li, Jinghui Xiu, Liang Yao, Qiuliang Li, Guannan Li, Xiaodong Li, Lu Zhang, Chunhong Ning, Wei Yun, Shizong Hu, Jingqi Huang. Comprehensive Profiling of The Immune Status of A Broad Range of *in vivo* Syngeneic Models to Support IO Development and to Accurately Predict Clinical Benefit of Therapy. Fortune Journal of Health Sciences. 7 (2024): 288-298.